JOURNAL OF APPLIED ELECTROCHEMISTRY 21 (1991) 1038–1046

REVIEWS OF APPLIED ELECTROCHEMISTRY 31

# Use of the polarographic method to measure wall shear stress*

T. J. HANRATTY

*University of Illinois, Urbana, IL 61801, USA*

Received 1 February 1991; revised 5 March 1991

The measurement of the current to a small polarized electrode mounted flush to the wall allows the determination of the local velocity field closer to a surface than any other method. This technique has found use in measuring wall shear stresses in boundary-layer flows and in studying the structure of turbulence in the viscous sublayer. The interpretation of measurements in the wake behind a cylinder or behind a large amplitude wave is not clear because large amplitude flow oscillations make present analysis of the performance of these wall electrodes inapplicable. Recent numerical work on the inverse mass transfer problem seems to offer an approach that can handle measurements in these difficult flows.

## 1. Introduction

Heyrovsky and his co-workers at the Charles University in Prague developed, over the period 1922–1935, the polarographic method which uses measurements of the current-voltage relation in an electrolysis cell for the qualitative and quantitative analysis of ions in solution [1, 2]. One of the electrodes (usually the cathode) is much smaller than the other so the current is determined by what is happening at this test electrode. A species in the solution reacts if the applied voltage exceeds a certain value. At high enough voltages the reaction proceeds rapidly enough that the current is controlled by the rate of mass transfer, and the concentration of the reacting species at the electrode surface is zero. This polarization conditions is identified by a plateau in the current-voltage curve.

Analytical chemists use this method under carefully controlled hydrodynamic conditions to determine the composition of a solution. The voltage at which polarization occurs identifies the presence of a species and the magnitude of the current is directly proportional to the concentration.

Engineers have utilized these techniques in an inverse manner. The chemistry is carefully controlled so that the current flowing measures properties of the flow field which are unknown. The first applications involved the determinatiion of rates of mass transfer [3, 4]. A particular advantage of the polarization technique in such studies is that it allows the measurement of the local time-varying mass transfer rate in a large mass transfer surface [5–12]. Ranz [13] was the first to use pology to measure local velocities. This work, as well as others that followed, showed that problems arise from electrode contamination.

The velocity gradient at a wall (or the shear stress, if the viscosity is known) can be determined by using a test electrode mounted flush with a wall. In this application the flowing fluid tends to keep the surface clean so that measurements are easier than with probes located in the body of a fluid. A number of laboratories (for example, the University of Illinois, the University of Nancy, Kyoto University, the Institute of Thermophysics at Novosibirsk, the University of Paris) have participated in the development of the wall electrode because it has opened up the possibility of making new fluid mechanics measurements [14–23].

The present paper reviews studies at the University of Illinois.

## 2. Description of the wall probe

The first work on the wall probe at the University of Illinois was done by Reiss [24, 25]. He became interested in the possibility of using electrochemical techniques to study turbulent flow close to a wall while trying to develop a method to introduce mass from a small wall source into a flow. Further improvements in the technique were made in a subsequent study by Mitchell [26]. In these works circular or rectangular nickel electrodes were glued into the wall of a pipe and ground flush. The reaction system was a dilute solution of potassium ferri- and potassium ferrocyanides (0.01 molar each) in a strong (2 molar) aqueous solution of sodium hydroxide. The sodium hydroxide acts as a low resistance vehicle for current flow and insures that the transfer to the cathode is controlled by diffusion. Under these conditions the flux of ferricyanide ion, $N$, to the surface of the cathode of area $A$ is related to the cell current, $I$, by the relation

$$N = I/m_e AF \quad (1)$$

* This paper was presented at the Workshop on Electrodiffusion Flow Diagnostics, CHISA, Prague, August 1990.



0021-891X/91 $03.00 + .12 

where $F$ is Faraday's constant and $m_e$ is the number of electrons involved in the reaction. A mass transfer coefficient, $K$, can be defined as

$$K = K(C_B - C_w) \tag{2}$$

where $C_B$ is the concentration of the reacting species in the bulk and $C_w$ is the concentration at the wall. At the polarization condition $C_w = 0$, so measurements of the current are directly proportional to the mass transfer coefficient and to the bulk concentration.

The relation of the mass transfer coefficient to the flow field is obtained by solving the mass balance equation for a rectangular electrode with its long side perpendicular to the direction of flow.

$$\frac{\partial C}{\partial t} + u\frac{\partial C}{\partial x} + v\frac{\partial C}{\partial y} + w\frac{\partial C}{\partial z} = D\left(\frac{\partial^2 C}{\partial x^2} + \frac{\partial^2 C}{\partial y^2} + \frac{\partial^2 C}{\partial z^2}\right) \tag{3}$$

The diffusion process is characterized by a large Schmidt number and, therefore, a very small thickness, $\delta_c$, for the concentration boundary layer. Under these conditions

$$u = S_x y \tag{4}$$

$$w = S_z y \tag{5}$$

$$v = \frac{1}{2}\left(\frac{\partial S_x}{\partial x} + \frac{\partial S_z}{\partial z}\right) y^2 \tag{6}$$

where $S_x$, $S_z$ are the components of the velocity gradient at the wall, and diffusion in the $x$- and $z$-directions can be neglected. For the electrode configuration used by Reiss and Mitchell and for cases in which $S_x$ is not close to zero the influences of the $v$ and $w$ velocity components can be ignored so that (3) simplifies to

$$\frac{\partial C}{\partial t} + S_x y\frac{\partial C}{\partial x} = D\frac{\partial^2 C}{\partial y^2} \tag{7}$$

If the flow is steady this equation can be solved to give

$$\frac{KL}{D} = 0.807Z^{1/3} \tag{8}$$

$$Z = \frac{S_x L^2}{D} = L^{+2}Sc \tag{9}$$

In the above, $L$ is the electrode length, $Sc$ is the Schmidt number and the '+' superscript indicates the quantity has been made dimensionless with wall parameters. The same equation can be used for circular electrodes if the effective length is set equal to 0.814 times the diameter [25]. Finite difference solutions for steady flow [18, 19, 27, 28] show that the error in using Equation 8, because of neglecting diffusion in the $x$- and $z$-directions, is less than 5% if $Z > 200$ with a rectangular electrode and if $Z > 1000$ with a circular electrode. A recent paper by Phillips [29] uses asymptotic methods to determine more general relations than Equation 8. Equation 8 was confirmed by Reiss [25] and by Mitchell [26] by measuring the time-averaged wall shear stress for laminar and turbulent flows in a 2.54 cm pipe.

A measure of the average thickness of the concentration boundary-layer over the electrode surface can be calculated from Equation 8 as

$$\frac{\delta_c}{L} = [0.807Z^{1/3}]^{-1} \tag{10}$$

This may be considered to be the measuring volume. For a range of $Z$ characteristic of turbulent flows a value of $\delta_c/L = 0.2$ to 0.03 is estimated from Equation 10. Electrodes with effective lengths as small as 0.1 mm have been used successfully. Therefore, typical thicknesses of the concentration boundary-layer over the electrode surface are 0.02 to 0.003 mm. Furthermore it is to be noted that (in contrast to other techniques) the measuring volume, $\delta_c$, decreases with increasing flow rate. This is an advantage since flow scales usually become smaller at large flows. The attactiveness of the electrochemical wall probe becomes apparent from the above considerations. Since it responds to velocity variations within the concentration boundary-layer, it has the capability of making fluid mechanics measurements closer to a solid surface than does any other technique. Since its behaviour can be determined by a solution of Equation 3 it need not be calibrated in properly designed experiments.

The polarized wall electrode has not had wider application because of difficulties associated with its use. Care must be taken in selecting the reaction system and materials of construction, and in designing the electrode. Contamination must be avoided and the electrode area needs to be known if the performance is to be determined analytically. Details regarding experimental procedures can be found in several reviews [15–18].

## 3. Measurements of time-averaged shear stresses

One of the main results from boundary-layer theory is the prediction of the wall shear stress variation around a body. Yet, the boundary-layer in many flows is so thin that conventional methods cannot be used to check theory. The experiments of Reiss and Mitchell suggested that electrochemical wall probes could be a valuable tool in this area of research. Consequently, two water tunnels were constructed to study flow around cylinders. One had a gravity feed [30]; it was designed by Dimopoulos to study flow at low Reynolds numbers. The other had a forced circulation; it was designed by Son [31] for large Reynolds numbers. Son developed the sandwich electrode shown in Fig. 1 for studies of two-dimensional boundary-layers. Two platinum electrodes, 25.4 mm × 0.127 mm, separated by 0.05–0.075 mm of insulation were embedded in the surface of a cylinder. The cylinder could be rotated so that the position of the sandwich electrodes could vary with respect to the oncoming flow. One of these is used as the test electrode. The current flowing to it gives the local wall shear stress. If the sudden activation of the

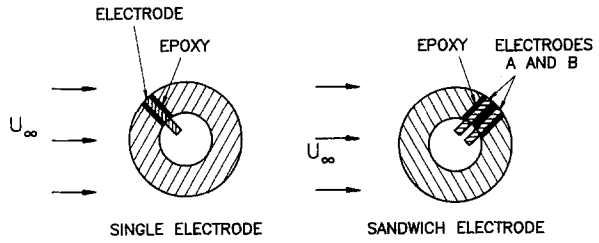


Fig. 1. Electrode configurations used to study flow around a cylinder.

other electrode causes a sudden change in the signal, then the test electrode is in the wake of the second electrode. By using this technique it is possible to determine the separation point for flow around a 1.9 cm cylinder to within 1°.

Measurements of the local magnitude of the time-averaged velocity gradient obtained by Son [31] are given in Fig. 2. These were calculated from the time-averaged current using (8) and made dimensionless with respect to the free stream velocity and the cylinder radius. The Reynolds number, $R$, appearing in the ordinate is defined in terms of the diameter of the cylinder. The separation point determined with the sandwich electrode is indicated with an arrow and the symbol $S$. The velocity gradient is positive in the region A and negative in the region B. In the early part of region C it is positive. However over most of C it changes direction as time goes on.

The region B, which existed for all of the Reynolds numbers studied by Son, suggests the existence of a separation bubble just behind the separation point. This is an interesting feature of these measurements since it had not been observed previously.

The measurements in region C are difficult to interpret. The flow is highly unsteady and the oscillations can be larger than the mean flow. Theory develolped in the previous section is not applicable, so the calculation of the mean magnitude of the velocity gradient with Equation 8 could be meaningless.

Measured values of the dimensionless velocity gradient prior to separation are presented in Fig. 3. As predicted by boundary-layer theory measurements at

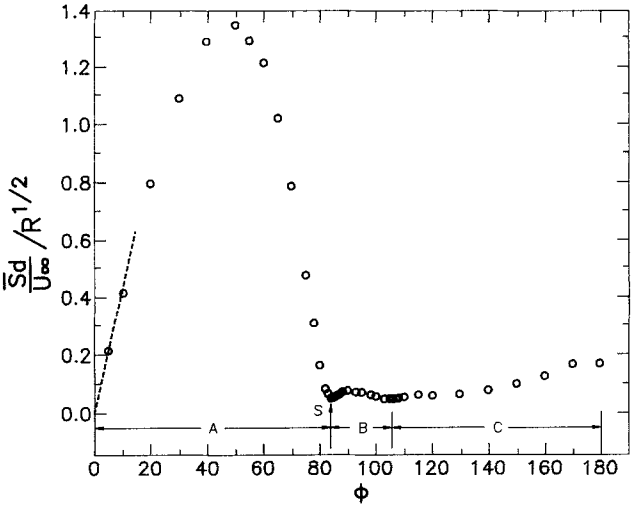


Fig. 2. Normalized wall velocity gradient, $R$ = 10000, 6.35 mm cylinder $d/h$ = 0.062, 27 gauge electrode.

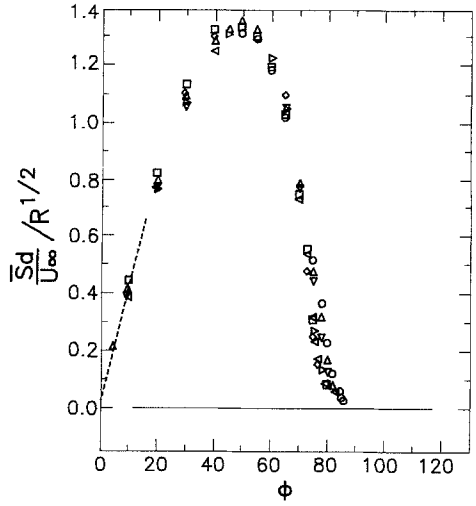


Fig. 3. Effects of Reynolds number in the wall velocity gradient distribution. $R$: (○) 5000, (△) 10000, (▽) 20000, (□) 40000, (△) 50000, (△) 70000, (◇) 1000000 and (- - -) boundary layer solution (potential flow).

different Reynolds numbers collapse on a single curve when the dimensionless velocity gradient is normalized with respect to $\sqrt{R}$.

According to the potential flow solution the velocity external to the boundary-layer is given by $V = 4xu_\infty/d$ in the neighbourhood of the front stagnation point, where $x$ is the distance from the front stagnation point, $d$ is the diameter of the cylinder and $u_\infty$ is the velocity at infinity. The boundary-layer solution based on this external flow is indicated by the dashed lines in Figs 2 and 3. It is seen that the velocity gradients in the neighbourhood of the front stagnation point are in good agreement with this solution.

The prediction of the complete profile of the wall velocity gradient from boundary-layer theory requires accurate pressure measurements, so that pressure gradients can be obtained. A calculation based on Hiemenz's pressure measurements at $R$ = 19000 is presented in Schlichting [32]. A comparison, between the calculation and measured velocity gradients at $R$ = 20000 is shown in Fig. 4. Good agreement is

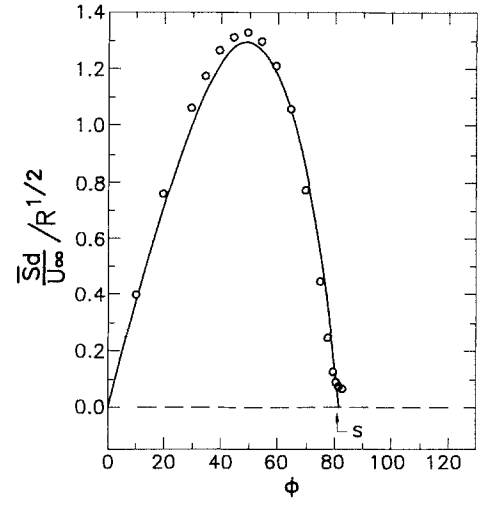


Fig. 4. Comparison between boundary layer calculations and measurements. $R$: 20000 (measurements), (——) 19000 (boundary layer solution).

obtained for both the location of the separation point and the variation of the surface velocity gradient.

The thicknesses of the boundary layers associated with the results shown in Fig. 2 are in the range 0.17 to 0.08 mm. The difficulty of using classical measuring techniques and the value of the electrochemical wall probe become evident.

Dimopoulos [30] carried out a study in which local mass transfer rates and local velocity gradients were measured in the same equipment. In the mass transfer studies the platinum cathode consisted of the entire cylinder surface. The current flow represented the total mass transfer to the cylinder. Local values of the mass transfer rate were measured by using a 0.50 mm round electrode embedded in, but isolated from, the main electrode. Local values of the velocity gradient were measured with platinum 0.50 mm × 12.5 mm rectangular electrodes embedded in an inert surface. Boundary-layer theory was used to calculate the local mass transfer rates from the measured profile of the velocity gradient. Figure 5 compares calculated mass transfer profiles at Reynolds numbers of 247, 293 and 339 with measurements at $R = 356$. The mass transfer rates are plotted in the ordinate as a Sherwood number divided by the product of the square root of the Reynolds number and the cube root of the Schmidt number.

The success of the experiments of Son and of Dimopoulos led to the use of wall electrodes to study flow around a sphere in beds of spheres [33–36] and of flow over wavy surfaces [37, 38]. To facilitate the studies in packed beds Karabelas [34] developed an electrode design that could give the direction of the wall shear stress, as well as the magnitude, in a three-dimensional boundary layer.

The motivation for the study of flow over wavy surfaces was the need to develop an understanding of wave generation. Theoretical work on this problem requires the forces imposed on a wave by the flow over it, i.e., the pressure and shear stress variation along the wave surface. The key theoretical problem is the prediction of the wave-induced variations of the Reynolds stress in the viscous wall region. Studies with small amplitude sinusoidal waves produce a sinusoidal variation of the wall shear stress [39, 40]. The measurements of the amplitudes and phases of the functions characterizing the stress variations provide a challenging test for theoretical models of the Reynolds stress close to a wall. For larger amplitude waves the stress profiles become non-sinusoidal and, for large enough waves, the flow separates [37, 38]. As was found for flow over a cylinder the use of the wall probes in the separated region is questionable because of the highly unsteady motion.

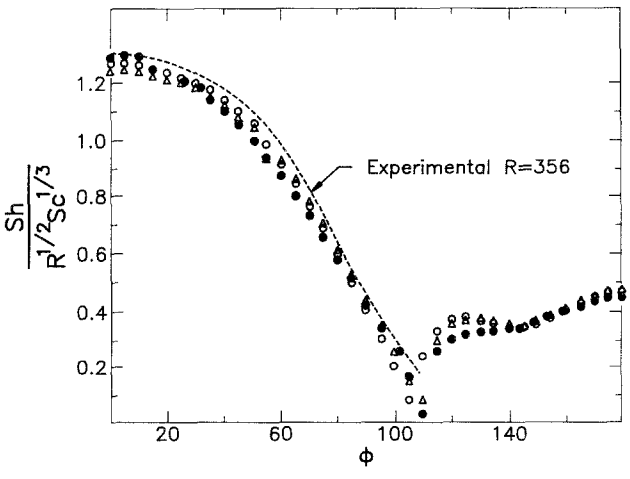


Fig. 5. Mass transfer variation around a circular cylinder predicted from the measured shear stress distribution and boundary-layer theory. $R$: (○) 339, (△) 293 and (●) 247.

Thorsness also made measurements of the mass transfer variation along small amplitude wavy surfaces [41]. These were used, in conjunction with the wall shear stress measurement, to interpret results on the stability of dissolving surfaces [42, 43].

## 4. Time response of wall probes

The results obtained in the separated regions behind cylinders and large amplitude waves indicate that the usefulness of electrochemical wall probes could be greatly expanded if their response to a time-varying flow were known.

For flow fluctuations with low frequency and with amplitudes that are not too large a pseudo-steady state assumption can be made whereby Equation 8 is used to relate the time varying shear rate at the wall to the measured time-varying mass transfer rate. In actual turbulent flows the concentration boundary layer over the electrode surface acts as a capacitance so that the mass transfer rate is not in phase with the velocity fluctuations and has a lower amplitude than would be predicted by the pseudo-steady state solution.

In an effort to understand the frequency response of electrodes used to measure turbulent flow fluctuations, Mitchell [26] suggested that the pseudo-steady state solution can be corrected by solving a linearized version of Equation 7,

$$\frac{\partial c}{\partial t} + \bar{S}_x y \frac{\partial c}{\partial x} + s_x y \frac{\mathrm{d}\bar{C}}{\mathrm{d}y} = D \frac{\partial^2 c}{\partial y^2} \qquad (11)$$

Here $\bar{C}$, $c$ and $\bar{S}_x$, $s_x$ are the time-averaged and fluctuating concentration and wall velocity gradient. The fluctuations in the velocity gradient and in the mass transfer coefficient can be represented as

$$s_x = \hat{s}_x \exp(\mathrm{i}2\pi nt) \quad k = k \exp(\mathrm{i}2\pi nt) \qquad (12)$$

where $\hat{s}_x$ is real and $\hat{k}$ is complex. The quasi-steady solution is

$$\hat{k}_s = \tfrac{1}{3}(\hat{s}_x/\bar{S}_x)\bar{K} \qquad (13)$$

and the frequency response can be represented as the relation of $\hat{k}$ to $\hat{k}_s$ (or $\hat{s}_x$); i.e., as a correction to the pseudo-steady state solution.

According to the pseudo-steady state solution the mean-square value of the fluctuations in the velocity gradient can be related to the mean-square in the fluctuations of the mass transfer coefficient by the

relation

$$\frac{(\overline{s_x^2})}{\bar{S}^2} = 9\frac{\bar{k}^2}{\bar{K}^2} \tag{14}$$

This can be corrected for the frequency response of the electrode if the spectral function of the mass transfer fluctuations, $W_k$, is measured. Thus, the spectral density function of the fluctuations in the velocity gradient is given as

$$W_s = 9\frac{\bar{S}^2}{\bar{K}^2}\frac{W_k}{A^2} \tag{15}$$

where

$$A^2 = \frac{|\hat{k}|^2}{\hat{k}_s^2} \tag{16}$$

is obtained from a solution of Equation 11.

Mitchell solved Equation 11 only for small frequencies. Fortuna [44] presented a solution of Equation 11 that is valid for all frequencies. Results on $A^2$ are presented in both references [44] and [15]. Mao [45] used the solution techniques of Fortuna to calculate the phase relation between $k$ and $s_x$.

Another way of presenting the solution of Equation 11 is as a transfer function $H(\mathrm{i}2\pi n)$ defined as

$$\hat{k} = H(\mathrm{i}2\pi n)\hat{s}_x \tag{17}$$

Expressions for $H(\mathrm{i}2\pi n)$ have been developed by a number of authors [21, 18, 46]. As pointed out by Py this approach has the possibility of developing an electronic circuit to represent $H(\mathrm{i}2\pi n)$ and, therefore, to convert time-varying currents from the electrolysis cell to a signal that directly represents the time-varying $s_x$.

A difficulty with the approach outlined above is that it is limited to cases for which $s_x/\bar{S}_x$ is small. It, thus, does not interpret the behaviour of wall probes in highly unsteady wakes, such as were observed by Son [31] and Zilker [38]. This is clearly seen in the calculations by Kaiping [47] and Pedley [48] of $k(t)$ for a sinusoidally varying $s_x(t)$. The linearized mass balance Equation 11, or the pseudo-steady state approximation, would predict a sinusoidally varying $k(t)$. The numerical solution of the non-linear balance, Equation 7, shows a very different behaviour for $s_x/\bar{S} \geqslant 0.5$. For cases in which the flow is reversing itself the $k(t)$ calculated from the pseudo-steady state approximation has little resemblance to the imposed $s_x(t)$.

These results prompted Mao to explore methods for analysing electrode measurements in a flow with large amplitude flow oscillations [49]. Considerably attention has been given to the problem of inverse heat conduction, as summarized by Beck [50]. The presence of a convection term in the mass or heat balance equation for wall probes, however, makes the analysis considerably more difficult. Moreover, when temporally reversing flow happens close to the wall the inverse problem is not unique.

Two methods were developed by Mao: In one of these a function for $S_x(t)$ with several unknown parameters is assumed. These parameters are selected through an iterative (finite difference) numerical scheme that calculates $K(t)$. The second method does not estimate $S_x(t)$ for the whole time domain. Instead, it is assumed the $S_x(t)$ for $t \leqslant t_k$ are known and that the predicted $K(t)$ for $t \leqslant t_k$ is a good fit to the measurements. Then $S_x(t_{k+1})$ is calculated at $t_{k+1}$ from experimental data on $K$ at $t_{k+1}$ and the knowledge about $S_x(t)$ for $t \leqslant t$. This is accomplished by an iterative method in which $S_x$ at $t_{k+1}$ is assumed and the mass balance equation is solved numerically to obtain $K$ at $t_{k+1}$. If this agrees with the measurement, then the assumed $S_x$ is correct. For cases in which a reversing flow exists additional information about the direction of flow is needed. This can be obtained from measurements with a sandwich of two electrodes.

Figure 6 gives an example of the periodic mass transfer signals calculated by Mao. These were obtained for a rectangular electrode with a time varying shear stress given by

$$S_x = \bar{S}_x + 2\bar{S}_x \cos(2\pi nt) \tag{18}$$

The term $Nu^* = Nu(L^{+2}Sc)^{-1/3}$ in Fig. 6 is a modified Nusselt number and $\omega^* = \omega^+ Sc^{1/3}L^{+2/3}$ is a modified dimensionless circular frequency. The analysis of the results in Fig. 6 by both of the methods outlined above gave Equation 18. These results suggest that the usefulness of wall electrodes can be expanded so that measurements of flows with large amplitude time-varying flows are possible.

## 5. Turbulent flows

The development of electrochemical techniques at the University of Illinois was, largely, motivated by an interest in the properties of a turbulent field close to a wall, beginning with a publication in 1956. In this paper we explored the notion that close to a wall the flow actively participates in the production of turbulence, and does not just passively respond to flow fluctuations in the outer flow [51]. The experiments by Reiss [24, 25] showed that wall electrodes offered the opportunity to obtain the type of quantitative information about turbulent flow close to a wall needed to

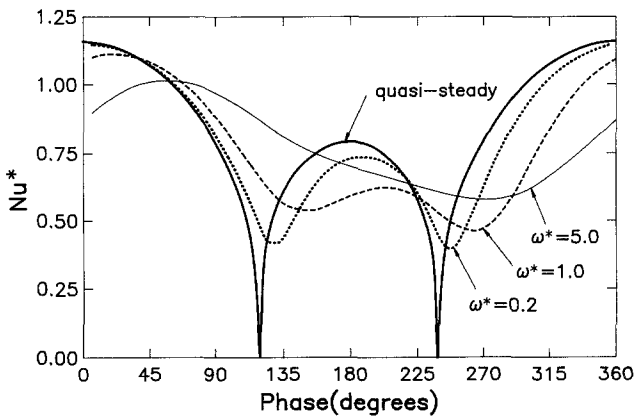


Fig. 6. Numerical calculations of the modified Nusselt number for shear rate $S = 1 + 2.0\cos(\omega^*\tau)$.

pursue this notion. Of particular interest were the results, obtained by Reiss, suggesting that turbulent flow at the wall is dominated by elongated eddies with very small spanwise scales.

These results seemed consistent with the streaky structures that had been observed when dye is injected at the wall [52, 53]. Mitchell [26] used the electrochemical wall probes to obtain quantitative information about the variation of the streamwise velocity fluctuations in the flow direction that seemed consistent with the suggestion by Kline and Runstadler that the dye streaks are regions of low velocity. Mitchell suggested that slant electrodes could be used to get information on the spanwise component of the velocity gradient at the wall. Sirkar [54, 55] pursued this idea and developed a probe consisting of two rectangular electrodes in a chevron arrangements that enabled him to obtain quantitative measurements. These showed that $s_z(t)$ is quite large, being of the order of $1/3\ s_x(t)$. This led Sirkar [10] to suggest that transport processes close to the wall are controlled by elongated eddies with circulation in a plane perpendicular to the direction of mean flow.

This idea was confirmed by experiments which made simultaneous time-varying measurements with an array of electrodes embedded in the wall and a rake of probes in the fluid [56–58].

Scales of the turbulence at the wall could be defined by measuring the space [26, 56, 59] or space-time [60, 21] correlation between pairs of wall probes separated by different distances. These show that spatial variations of the flow scale with wall parameters in the spanwise direction and with a combination of wall parameters and bulk parameters in the streamwise direction. The study of spatial correlations by Finnicum [59] followed a suggestion by Py [21] that the limiting behaviour of velocity fluctuations normal to the wall could be determined from conservation of mass (Equation 5) by measuring the derivatives of $s_x$ in the $x$-direction and of $s_z$ in the $z$-direction with two pairs of electrodes separated by very small distances. Measurements with multiple wall electrodes in the presence of drag-reducing polymers [61–63] show that increases in drag-reduction are correlated to increases in the spanwise scale of the wall eddies.

In making turbulence measurements with wall electrodes one is concerned with spatial averaging over the electrode surface and with the time response of the concentration boundary-layer. Spatial averaging puts a severe limitation on the use of wall electrodes because of the small scale of turbulence in the spanwise direction. Mitchell [26] explored methods to correct measurements of the mean-square of the fluctuations for spatial averaging. This study shows that the spatial extent of the electrode in the spanwise direction needs to be less than 8 wall units ($W^+ < 8$) for the averaging error to be less than 5%.

Measurements of $s_x$ by Mitchell [26] were corrected for spatial averaging but not for frequency response. These gave values of $(\overline{s_x^2})^{1/2}$ equal to $0.32\bar{S}_x$. Fortuna [44] used the linear frequency response calculation to correct measurements with small circular electrodes and obtained $(\overline{s_x^2})^{1/2} = 0.35\bar{S}_x$. Sirkar [55] carried out experiments in a specially built large diameter (20.3 cm) pipe for which no spatial or temporal corrections had to be made. He obtained $(\overline{s_x^2})^{1/2} = 036\bar{S}_x$. A value of $(\overline{s_x^2})^{1/2} = 0.35\bar{S}_x$ was later obtained by Mao [45] in the same equipment. In contrast to what Mitchell [26] suggested earlier, Sirkar [55, 63] found that the spectrum of $s_x$ scales with wall parameters.

The large value of the measured root-mean-square of $s_x$ leads to concern about the linear analysis that has been used to calculate the frequency response of wall probes in turbulent flows. In addition, $s_x$ has large positive skewness so that large positive excursions of the order of $\bar{S}_x$ are observed. Consequently, the second inverse method described in the previous section was used by Mao [64] to correct measurements. The experiments were conducted in a 5 cm pipe. A circular electrode of diameter 0.0127 cm was used. The dimensionless length of this electrode under the experimental conditions was 5 wall units, so it was felt that no correction had to be made for spatial averaging. The data were digitized and the value $s_x$ corresponding to each point was calculated with the numerical algorithm. This then gave a signal representing the time-variation of $s_x$.

This signal was analysed to obtain (what are quite likely the best at the University of Illinois) measurements of the probability distribution and the frequency spectrum of $s_x$. These gave $(\overline{s_x^2})^{1/2} = 0.37\bar{S}_x$, a skewness of 0.96 and a flatness of 4.2. A comparison of the frequency spectra obtained using linear and non-linear analyses reveals that the linear theory correction underestimates the energy content of large amplitude high frequency fluctuations.

In making measurements of spanwise velocity fluctuations Sirkar [55] used two 0.0762 mm × 1.016 mm rectangular electrodes. These electrodes had their long side at an angle of 15° to the direction of mean flow. The maximum spanwise spread of the pair was 0.64 mm. The sum of the signals from these gave $s_x$. The difference gave $s_z$. The angle between the electrodes limited the measurements only to flows making an angle of less than 15° to the direction of flow. Consequently, the selection of the angle between the two electrodes was a compromise between making the dimensions in the spanwise direction small enough that spatial averaging is having a small effect, yet large enough that sufficient sensitivity to $s_z$ variations is obtained. As a consequence of this compromise it is quite possible that the measurement of $s_z$ by Sirkar is on the low side.

Py [28, 21, 27] explored the use of two semicircular or two rectangular electrodes with a small layer of insulation between them. In both cases the electrode pair is oriented so that the insulation layer is in the direction of mean flow. This design is attractive because it is so compact. However, considerable difficulties are encountered in fabrication, in controlling the thickness of the insulation, and in analysing for the effect of the insulation.

## 6. Flows with imposed oscillations

Studies were carried out by Mao and Finnicum in which a sinusoidal pressure gradient was imposed on the mean pressure gradient forcing a turbulent fluid through a 20.32 cm pipe [45] and through a 5.08 cm pipe [66]. The imposed oscillations were small so that the phase-averaged velocity showed a sinusoidal variation. A principal motivation for these sutides was to understand how drag on the wall can be affected. Finnicum and Mao used electrochemical wall probes to measure the mean and the phase-averages of the wall shear stress.

Special considerations had to be given to the design of the electrodes and to the interpretation of the results. For imposed oscillations of high frequency the disturbance velocity is flat over the whole pipe cross-section with the exception of the thin Stokes layer at the wall, whose thickness is defined as

$$\delta_s^+ = \left(\frac{2}{\omega^+}\right)^{1/2} \tag{19}$$

Of particular interest in these studies were imposed frequencies equal to the median frequency of the turbulence, or higher, $\omega^+ \geqslant 0.056$, so $\delta_s^+$ could be smaller than the thickness of the viscous sublayer, $\delta_v^+ = 5$.

Since the concentration boundary-layer over the electrode should be smaller than the Stokes layer, Equations 19 and 10 require that

$$L^+ < 0.11(\omega^+)^{-3/2} Sc \tag{20}$$

Also, in order that the mathematical representation by Equation 7 be valid it is necessary that $\delta_c^+ < 5$ over the whole electrode. This requires that

$$L^+ < 5Sc \tag{21}$$

The neglect of diffusion in the flow direction requires that

$$L^+ > 14Sc^{-1/2} \tag{22}$$

if the error in using Equation 8 is to be less 5%.

The linear-theory analysis outlined in section 4 suggests that

$$\omega^+ Sc^{1/3} L^{+2/3} \leqslant 1 \tag{23}$$

if it is desired that the error in using Equation 8 to calculate the amplitude of the phase-average of the wall shear stress variation be less than 5%. The criterion to avoid corrections on the phase angle is more restrictive:

$$\omega^+ Sc^{1/2} L^{+2/3} \leqslant 0.3 \tag{24}$$

for an error of less than 5°. Mao and Finnicum were able to design their experiments so that only a correction on the phase needed to be made. However, in order to do this it was necessary that the ratio of the amplitude of the variation of the phase-averaged shear stress to the time-averaged shear stress be kept less than 0.6. In order to study larger imposed oscillations it would be necessary to use the non-linear analysis outlined in section 4.

## 7. Effect of Schmidt number or Prandtl number

The strong effect of Prandtl number or Schmidt number on probe performance becomes evidence in the above discussion. If $Sc = 1000$, which might be realized with an electrochemical probe, Equations 21 and 22 indicate $0.44 < L^+ < 5000$.

If $L^+ = 0.44$ is used in Equation 20 it is found that the thinness of the Stokes layer is not a limitation in that frequencies as high as $\omega^+ = 40$ can be studied without violating the equation. From Equation 24 it is found, with $L^+ = 0.44$, that frequencies as high as $\omega^+ = 0.052$ can be used without correcting for frequency response of the scalar boundary-layer.

A consideration of Equations 23 and 24 suggests that limitations imposed by the frequency-response of the scalar boundary-layer would be less restrictive for flush mounted thermal probes, but this is not the case. If one considers a thermal probe in a water flow, then $Pr = 5$. Equations 21 and 22 indicate $6.3 < L^+ < 25$ should be used. This is clearly more restrictive than for $Sc = 1000$ since a single probe would be able to satisfy these restrictions over a narrow range of flows.

If the influence of the Stokes layer is considered for $L^+ = 6.3$, it is found that frequencies as high as $\omega^+ = 0.20$ can be studied without violating Equation 20. From Equation 20 for $L^+ = 6.3$, it is found that frequencies as high at $\omega^+ = 0.052$ can be used without correcting the phase for the frequency response of the scalar boundary-layer. Thus, even though this equation suggests a more serious effect of frequency response at large $Sc$, the restriction on $\omega^+$ is the same. This is because Equation 22 requires the use of probes of larger length for $Pr = 5$ than for $Sc = 1000$.

The conclusion from these considerations is that, from the viewpoint of restrictions imposed by the time response of the scalar boundary-layer, mass transfer probes are superior to thermal probes. The superiority is even greater, if one considers that in the use of thermal probes one also has to consider the transient heating of the substrate on the frequency response. Such an effect is not present in the case of electrochemical probes.

## 8. Conclusion

Polarized wall electrodes are capable of measuring the velocity extremely close to a boundary. Furthermore the equations defining their performance are well defined so that, in principle, no calibrations are needed. Consequently they have found application in research studies of boundary-layer flows and of turbulent flows over solid boundaries. Although considerable work has been done in a number of laboratories in developing these techniques there are still areas of study that have the possibility of increasing the usefulness of these wall probes:

1. The expansion of computer capability opens up the

opportunity of interfacing computers more strongly with experiments. This will require fast numerical algorithms which solve the time-dependent multi-dimensional mass balance equation over the electrode configuration being used. The work by Mao [49, 64] in this direction is encouraging. The principal benefit, if successful, would be the capability to use wall electrodes in poorly understood separated flows.

2. The use of complicated electrode configurations is often limited because of the difficulty of fabricating them to exact specificiations. Better techniques, such as used in building printed circuits, should be explored.

3. The electrochemical systems most widely used are the ferrocyanide–ferrocyanide reaction on nickel or platinum electrodes (with sodium hydroxide or potassium chloride as the neutral electrolyte) or the iodine reaction on platinum electrodes (with potassium iodide as the neutral electrolyte). Both have disadvantages associated with usage in large flow systems. Other chemical reactions should be explored. In particular, if an oxygen electrode could be used then application in a sea water environment might be possible.

## Acknowledgement

This work was supported by the National Science Foundation under Grant CBT 88-00980 and by the Office of Naval Research under Grant N00014-82 K0324.

## References

[1] J. Heyrovsky, *Chem. Listy* **16** (1922) 256.
[2] J. Heyrovsky, 'Polarographie', Springer, Vienna (1941).
[3] C. S. Lin, E. B. Denton, H. S. Gaskill and G. L. Putnam, *Ind. Eng. Chem.* **43** (1951) 2136–43.
[4] E. J. Fenech and C. W. Tobias, *Electrochemica Acta* **2** (1960) 311–25.
[5] P. Grassman, N. Ibl and J. Trüb, *Chemie-Ingenieur-Technik* **8** (1961) 529–33.
[6] P. V. Shaw, L. P. Reiss and T. J. Hanratty, *AIChE Journal* **9** (1963) 362–4.
[7] G. Schütz, *Int. J. Heat Mass Transfer* **7** (1964) 1077–82.
[8] P. V. Shaw and T. J. Hanratty, *AIChE Journal* **10** (1964) 475–82.
[9] H. G. Dimopoulos and T. J. Hanratty, *J. Fluid Mech.* **33** (1968) 303–19.
[10] K. K. Sirkar and T. J. Hanratty, *ibid.* **44** (1970) 589–603.
[11] D. A. Shaw and T. J. Hanratty, *AIChE Journal* **23** (1977) 28–37.
[12] *Idem, ibid.* **23** (1977) 160–9.
[13] W. E. Ranz, *ibid.* **4** (1958) 338.
[14] T. J. Hanratty, in 'Heat and Mass Transfer in Flows with Separated Regions' (edited by Z. Zaric) Pergamon Press, Oxford (1972).
[15] T. J. Hanratty and J. A. Campbell, in 'Fluid Mechanics Measurements' (edited by R. J. Goldstein), Hemisphere, Washington (1983) pp. 559–611.
[16] T. Mizushina, 'Advances in Heat Transfer', Vol. 7, Academic Press, New York (1971) 87–161.
[17] S. S. Kutateladze, 'Gradient and Separated Flows', Academy of Sciences of the USSR, Siberian Department Institute of Thermophysics (1976).
[18] V. Ye Nakoryyakov, A. P. Burdukov, O. N. Kashinsky and P. I. Geshev, Electro-Diffusion Method of Investigation into Local Structure of Turbulent Flows, Academy of Sciences of the USSR, Siberian Branch, Institute of Thermophysics (1986).
[19] G. Cognet, Thesis, Nancy (1968).
[20] M. Lebouche, Thèse Doctrat ès Sciences, Nancy (1968).
[21] B. Py, *J. Heat Mass Transfer* **16** (1973) 129–44.
[22] C. Deslouis, Thèse de Doctorat d'État, Universitairé Pierre et Marie Curie, Paris (1975).
[23] B. Tribollet, Thèse, Universitairé Pierre et Marie Curie, Paris (1978).
[24] L. P. Reiss and T. J. Hanratty, *AIChE Journal* **9** (1962) 245.
[25] L. P. Reiss and T. J. Hanratty, *ibid.* **9** (1963) 154.
[26] J. E. Mitchell, *J. Fluid Mech.* **26** (1966) 199–221.
[27] B. Py, 'Les Proprietes Generales des Transducteurs Electrochimique Scindes', Euromech. 90 Proc. (1977).
[28] B. Py and J. Gosse, Sur la Realisation dúne Sonde en Paroi Sensible a la Vitesse et a la Direction de l'Ecoulement, *C. R. Acad. Sci.* **269 A** (1969) 401–3.
[29] C. G. Phillips, *Q. J. Mech., Appl. Math.* **43** (1990) 135–59.
[30] H. G. Dimopoulsos and T. J. Hanratty, *J. Fluid Mech.* **30** (1968) 303–19.
[31] J. S. Son and T. J. Hanratty, *ibid.* **85** (1969) 353–68.
[32] H. Schlichting, 'Boundary-Layer Theory', 4th ed., McGraw-Hill, New York (1960).
[33] K. R. Jolls and T. J. Hanratty, *Chem. Eng. Sci.* **21** (1966) 1185–90.
[34] A. J. Karabelas and T. J. Hanratty, *J. Fluid Mech.* **34** (1968) 159–62.
[35] K. R. Jolls and T. J. Hanratty, *AIChE Journal* **15** (1969) 199–205.
[36] A. J. Karabelas, T. H. Wegner and T. J. Hanratty, *Chem. Eng. Sci.* **28** (1973) 673–82.
[37] V. P. Zilker, G. W. Cook and T. J. Hanratty, *J. Fluid Mech.* **82** (1977) 29–51.
[38] V. P. Zilker and T. J. Hanratty, *ibid.* **90** (1979) 257–71.
[39] C. B. Thorsness, P. E. Morrisroe and T. J. Hanratty, *Chem. Eng. Sci.* **30** (1978) 579–92.
[40] J. Abrams and T. J. Hanratty, *J. Fluid Mech.* **151** (1985) 443–55.
[41] C. B. Thorsness and T. J. Hanratty, *AIChE Journal* **25** (1979) 686–97.
[42] C. B. Thorsness and T. J. Hanratty, *ibid.* **25** (1979) 697–701.
[43] T. J. Hanratty, *Annual Reviews of Fluid Mechanics* **13** (1981) 251–2.
[44] G. Fortuna and T. J. Hanratty, *Int. J. Heat Mass Transfer* **14** (1971) 1499–507.
[45] Z. Mao and T. J. Hanratty, *J. Fluid Mech.* **170** (1986) 545–64.
[46] A. Ambari, C. Deslouis and B. Tribollet, *Int. J. Heat Mass Transfer* **29** (1986) 35–45.
[47] P. Kaiping, *ibid.* **26** (1983) 545–57.
[48] T. J. Pedley, *J. Fluid Mech.* **78** (1976) 513–34.
[49] Z. Mao and T. J. Hanratty, *Int. J. Heat and Mass Transfer* **34** (1991) 281–290.
[50] J. V. Beck, B. Blackwell and C. R. St Clair, Jr., 'Inverse Heat Conduction, Ill-Posed Problems', John Wiley & Sons, New York (1985).
[51] T. J. Hanratty, *AIChE J.* **2** (1956) 359–62.
[52] S. Corrsin, 'Some Current Problems in Turbulent Shear Flows', Naval Hydrodynamics, Publication 515, National Academy of Sciences, National Research Council, Washington, D.C. (1957) chapter 15.
[53] S. J. Kline and P. W. Runstadler, *Trans ASME (Ser E)*, no. 2 (1959) 166.
[54] K. K. Sirkar and T. J. Hanratty, *Ind. Eng. Chem. Fundamentals* **8** (1969) 198.
[55] K. K. Sirkar and T. J. Hanratty, *J. Fluid Mech.* **44** (1970) 605.
[56] M. K. Lee, L. D. Eckelman and T. J. Hanratty, *ibid.* **66** (1974) 17–33.
[57] C. Nikolaides, K. K. Lau and T. J. Hanratty, *ibid.* **130** (1983) 91–108.
[58] J. H. A. Hogenes and T. J. Hanratty, *ibid.* **124** (1982) 363–90.
[59] D. S. Finnicum and T. J. Hanratty, *Phys. Fluids* **28** (1985) 1654–58.
[60] K. K. Sirkar, MS thesis, University of Illinois, Urbana (1966).
[61] G. Fortuna and T. J. Hanratty, *J. Fluid Mech.* **53** (1972) 575–86.
[62] L. D. Eckelman, G. Fortuna and T. J. Hanratty, *Nature Physical Science* **236** (1972) 94–6.
[63] L. G. Chom, D. T. Hatziavramidis and T. J. Hanratty, *The Physics of Fluids* **20** (1977) S112–S119.

[64] Z. Mao and T. J. Hanratty, *Experiments in Fluids* **11** (1991) 65–73.
[65] P. Duhamel and B. Py, Caratere Intermittent de la Sous-Couche Visqueuse AAAE 9e, Colloque D'Aerodynamique Appliquée, Paris (1972).
[66] U. S. Finnicum and T. J. Hanratty, *Physico-Chemical Hydrodynamics* **10** (1988) 585–5.